Load transportation using rotary-wing UAVs

Rafael José Figueiras dos Santos
rafael.j.f.santos@tecnico.ulisboa.pt

Instituto Superior Técnico, Lisboa, Portugal

December 2015

Abstract

The problem of slung load transportation by a quadrotor is addressed. It is assumed that the load is a point mass, and the cable is always stretched and connected to the center of gravity of the quadrotor. Dynamic models are derived for the quadrotor alone and for the system consisting of the UAV and the load. Quadrotor position controllers are developed and tested. These controllers may be used with the multi-body system, with the load acting as a disturbance. Controllers that take into account the dynamics of the load are also designed. Two controllers are presented, one based on the Backstepping technique and another based on the Singular Perturbation Method. Stability proofs for every controllers are present. Simulation and experimental results are presented.

Keywords: Unmanned Aerial Vehicles, slung load transportation, Non-linear control, trajectory tracking

1. Introduction

An UAV is a platform able to navigate and track trajectories with great accuracy. Some tasks are better performed by these vehicles than by human operators. For example, they are capable of going closer to an infrastructure and analyse it with better results while, at the same time, are saving human lives from being endangered. Other applications involve search and rescue missions, environmental monitoring or surveillance.

In this work, a particular type of UAV is studied, which is the quadrotor. It is a Vertical Take-Off and Landing (VTOL) vehicle, usually relatively small, that can go to inaccessible areas to humans or other kind of vehicles. Unlike fixed-wing airplanes, they can move in its vertical plane, and are able to hover or fly at low speeds. In addition, they do not require a runway to take-off or land.

Since the motion control problem in free flight of a quadrotor is reaching its maturity, the interaction between these vehicles and the environment is becoming a topic of high interest to researchers. Grasping objects [9] and building structures [8] are some examples. Another interaction, which is the main topic of this article, is load transportation. This can be done by a single or by multiple quadrotors.

There is a huge amount of applications for load transportation by an UAV. Experiments in the beach with drones carrying floatation devices to drowning people are being executed. UAVs may also be of extreme importance in the event of a catastrophe like an earthquake, a tsunami or a storm. Their agility allows them to reach remote and inaccessible sites. Delivering materials to offshore oil rigs or houses in mountainous regions is another possibility.

One way to carry a load is using a gripper directly connected to the UAV. This gripper grabs an object and keeps it fixed in relation to the drone, close to its center of gravity. The drawback of this approach is that it increases the inertia of the system, so the attitude manoeuvrability deteriorates. This makes the quadrotor less robust to reject perturbations. An alternative is to suspend the load using a cable, what keeps the attitude manoeuvrability performance. This is the approach used in this work.

Due to the characteristics of a quadrotor and to the several number of applications regarding load transportation, this problem has been acquiring a lot of interest in the scientific community.

The problem of controlling the position of a quadrotor has been addressed in several different ways. Classical control techniques have been studied, like the use of a PID controller, in [7]. Nonlinear techniques have also been considered. In [6], a geometric control for position tracking of a quadrotor is proposed. The design and stability analysis of a hierarchical controller for UAVs, using singular perturbation theory is discussed in [3].

Regarding the load transportation problem, [10] implemented an adaptive controller considering changes in the center of gravity and also an optimal trajectory generation based on dynamic programming for swing-free maneuvering. Also based on dynamic programming, [11] ensures swing-free trajectory tracking.

Geometric control for tracking load arbitrary trajectories, while allowing the load to potentially undergo large dynamics swings has been studied in [12]. Some

other modeling and control techniques are in [2].

2. Dynamic Modeling

In this section, nonlinear dynamic models are derived using Newtonian Mechanics for the quadrotor alone and for the quadrotor with suspended load.

2.1. Quadrotor Model

Consider a quadrotor of mass m_Q and inertia matrix J_Q, a reference frame denoted by $\{\mathcal{Q}\}$, attached to the quadrotor with origin at its center of mass, and an inertial reference frame $\{\mathcal{I}\}$, fixed in the environment. Quadrotor's position and velocity, with respect to $\{\mathcal{I}\}$, are given by x_Q and v_Q, respectively. The orientation $\{\mathcal{Q}\}$ with respect to $\{\mathcal{I}\}$ is described by the rotation matrix R, whereas the angular velocity of $\{\mathcal{Q}\}$, w.r.t. $\{\mathcal{I}\}$, expressed in $\{\mathcal{Q}\}$, is denoted by Ω.

Using Newton's laws, and assuming that the forces applied to the quadrotor are due to gravity and thrust, the translational motion can be described by

$$\dot{x}_Q = v_Q \tag{1a}$$

$$m_Q \ddot{x}_Q = -f R e_3 + m_Q g e_3 \tag{1b}$$

where f denotes the scalar thrust force that results from adding the thrust forces generated by all four rotors, $e_3 = [0\ 0\ 1]^T$, and g is the gravitational acceleration. For the rotational motion, Euler's equation can be written in terms of the body-fixed angular velocity, yielding

$$J_Q \dot{\Omega} + \Omega \times J_Q \Omega = M \tag{2}$$

where M is the three-dimensional torque vector that results from a combination of differences between the thrust forces generated by each of the four rotors. To derive an expression for the kinematics of rotation, notice that for a generic rotation matrix R, the matrix $R^T \dot{R}$ is a skew-symmetric matrix, i.e., it can be written as

$$R^T \dot{R} = S(a) \tag{3}$$

where $a \in \mathbb{R}^3$ and $S(a)$ denotes the skew-symmetric matrix given by

$$S(a) = \begin{bmatrix} 0 & -a_z & a_y \\ a_z & 0 & -a_x \\ -a_y & a_x & 0 \end{bmatrix}$$

As shown in [5], given the definitions of R and Ω, the vector a is given exactly by Ω. Finally, from Equation (3) it follows that

$$\dot{R} = R S(\Omega) \tag{4}$$

2.2. Quadrotor with Suspended Load Model

The dynamics of a quadrotor with a cable suspended load, where the load is a point mass, is discussed in this section. The system and the inertial reference frame $\{\mathcal{I}\}$ used are represented in Figure 1. The forces actuating in the quadrotor and in the load are also represented. The load has a mass m_L and its position and velocity, with respect to $\{\mathcal{I}\}$, are given by x_L and v_L respectively. Its angular velocity in the quadrotor fixed frame is ω, and q is the unit vector that points from the UAV to the load. Let T denote the magnitude of the tension force exerted by the load in the quadrotor and l the length of the cable that connects both bodies, such that

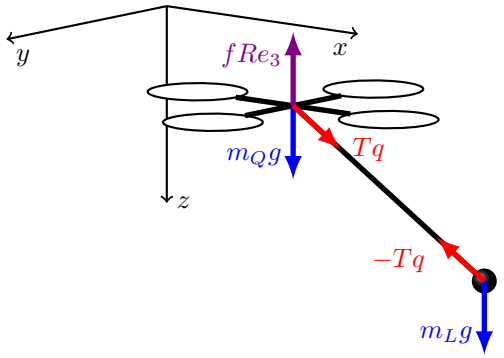

Figure 1: Quadrotor with cable suspended load and the coordinate system used.

$$x_L = x_Q + lq \tag{5}$$

The equations that describe the rotational motion of the quadrotor remain the same as before, i.e., are given by (2) and (4). Given that x_Q and x_L are related by (5), to describe the translational motion of the system, we can consider these two positions or alternatively either x_Q or x_L together with q. Since we are interested in controlling directly the position of the load, it is convenient to consider x_L and q and their derivatives as states of the system. For that purpose, let v_L denote the load velocity expressed in the inertial frame, such that

$$\dot{x_L} = v_L \tag{6}$$

Notice also that, assuming that the cable is stretched, the kinematics of q can be described by

$$\dot{q} = \omega \times q \tag{7}$$

where ω includes the components of the angular velocity orthogonal to q, i.e., $q^T \omega = 0$.

To obtain the equations for the dynamics, consider as starting point the Newton laws applied to both the quadrotor and load, which are interconnected by the tension force applied along the direction q, i.e.

$$m_Q \ddot{x}_Q = -f R e_3 + m_Q g e_3 + Tq \tag{8a}$$

$$m_L \ddot{x}_L = m_L g e_3 - Tq \tag{8b}$$

Summing up these equations

$$m_Q \ddot{x}_Q + m_L \ddot{x}_L = -f R e_3 + m_Q g e_3 + m_L g e_3 \tag{9}$$

Recalling (5) and taking the time derivative twice yields

$$\dot{v}_L = \dot{v}_Q + l\ddot{q} \tag{10}$$

Combining equations (9) and (10), it follows that

$$(m_Q + m_L)(\dot{v_L} - ge_3) = -fRe_3 + m_Q l\ddot{q} \quad (11)$$

To eliminate the term on $\ddot{q}$, (8) and (10) are used to obtain

$$l\ddot{q} = \dot{v_L} - \dot{v_Q} = -\frac{Tq}{m_L} + \frac{fRe_3}{m_Q} - \frac{Tq}{m_Q} \quad (12)$$

Multiplying by $S(q)^2 = qq^T - I$, in order to eliminate the term in T, we obtain

$$qq^T l\ddot{q} - l\ddot{q} = qq^T \frac{fRe_3}{m_Q} - \frac{fRe_3}{m_Q} \quad (13)$$

Differentiating (7) twice and multiplying by q^T one obtains $q^T\ddot{q} = q^T S(w)\dot{q}$, so (13) becomes

$$m_Q l\ddot{q} = -m_Q l(\dot{q}^T\dot{q})q - (q^T fRe_3)q + fRe_3 \quad (14)$$

Replacing in (11), the final equation for v_L is obtained

$$(m_Q + m_L)(\dot{v_L} - ge_3) = -\left(q^T fRe_3 + m_Q l(\dot{q}^T\dot{q})\right)q \quad (15)$$

Now, just an equation for ω is left to be found. It is obtained multiplying Equation (14) by $S(q)$, and by knowing that q is orthogonal to ω and $\dot{\omega}$

$$m_Q l\dot{\omega} = q \times fRe_3 \quad (16)$$

The equations can be split into three different groups. The first one describes the translational motion of the load and is the following

$$\begin{cases} \dot{x}_L = v_L & (17) \\ \dot{v}_L = -\dfrac{\left(q^T fRe_3 + m_Q l(\omega^T\omega)\right)q + ge_3}{m_Q + m_L} & (18) \end{cases}$$

The second group describes the rotational motion of the load in relation to the quadrotor

$$\begin{cases} \dot{q} = -S(q)\omega & (19) \\ \dot{\omega} = \dfrac{S(q)fRe_3}{m_Q l} & (20) \end{cases}$$

The last group describes the rotational motion of the quadrotor and is given by

$$\begin{cases} \dot{R} = RS(\Omega) & (21) \\ \dot{\Omega} = J_Q^{-1}(M - \Omega \times J_Q\Omega) & (22) \end{cases}$$

3. Quadrotor Position Control

In this section, the problem of the position control of a rotary-wing UAV is addressed. We will start with a Backstepping Controller [5]. Using this method, the translational and rotational dynamics subsystems, derived in Section 2.1, are considered, one at a time, and stabilizing controllers are designed for each one of them. After that, an Hierarchical controller is derived, using the time-scale separation principle. This leads to a simpler controller, since it avoids the calculation of some derivatives.

3.1. Nonlinear Backstepping Controller

Using the following control law

$$fr_3^* = m_Q(ge_3 - u) \quad (23)$$

And replacing in the v_Q dynamics equation, the translational equations become

$$\begin{cases} \dot{x}_Q = v_Q & (24) \\ \dot{v}_Q = u - \dfrac{f}{m_Q}(r_3 - r_3^*) & (25) \end{cases}$$

This system is equivalent to a double integrator, when $r_3 = r_3^*$. To be able to do trajectory tracking, the following u is selected

$$u = -K_p\widetilde{x}_Q - K_v\dot{\widetilde{x}}_Q + D^2x_Q^* \quad (26)$$

where $\widetilde{x}_Q = x_Q - x_Q^*$, x_Q^* is the desired trajectory, and D^n denotes the n-th order time derivative. Solving (23) for f and r_3^* and choosing the positive thrust solution, we obtain

$$f = m_Q||ge_3 - u|| \quad (27)$$

$$r_3^* = \frac{ge_3 - u}{||ge_3 - u||} \quad (28)$$

which is well-defined provided that $ge_3 - u \neq 0$.

At this point, an expression for the actuation f, which guarantees the stability of the system, is known, and so is the corresponding desired value for the vector r_3. We are now in conditions to design the attitude controller. The goal of this control loop is to guarantee the convergence of r_3 to r_3^*. It was shown in Section 2.1 that $\dot{R} = S(R\Omega)R$. Multiplying both members by e_3 and rearranging the equation, we obtain

$$\dot{r}_3 = -S(r_3)R\Omega \quad (29)$$

We will consider that the actuation is done in Ω, such as in the real model used for the experimental tests. Therefore, this is the only equation considered for attitude dynamics.

Applying Lyapunov stability theory based on the backstepping tecnhique, it can be shown that the angular velocity input that stabilizes the system is

$$\Omega = R^T(K_{r_3}S(r_3)r_3^* + S(r_3^*)\dot{r}_3^*) \quad (30)$$

where the first derivative of r_3^* is given by

$$\dot{r}_3^* = \Pi_{r_3^*}\frac{\dot{U}}{||U||} \quad (31)$$

with $U = ge_3 - u$ and $\dot{U} = -\dot{u}$.

3.2. Hierarchical Nonlinear Controller

Hierarchical control builds on the principle of having a time-scale separation between the slow states of a outer-loop system and the fast states of a inner-loop system. It can be shown that when the inner-loop system is sufficiently fast with respect to the outer-loop system, then stability of the combined system is guaranteed.

In this section, we will derive lower bounds for the inner-loop gains to ensure stability of the overall system. During the analysis, the time-scale separation concept will be taken into account, that will allow the use of some simplifying assumptions in the design of the controller.

Consider first the error system for the translational motion with states given by $\widetilde{x}_Q = x_Q - x_Q^*$ and $\widetilde{v}_Q = v_Q - v_Q^*$. The dynamics equations are

$$\begin{cases} \dot{\widetilde{x}}_Q = \widetilde{v}_Q & (32) \\ \dot{\widetilde{v}}_Q = \dot{v}_Q - v_Q^* = -\dfrac{fr_3}{m_Q} + ge_3 - \dot{v}_Q^* & (33) \end{cases}$$

Similarly to approach followed in Section 3.1, we define a desired thrust vector

$$F^* = f^* r_3^* = m_Q(ge_3 - u) \tag{34}$$

Such that r_{3*} is given by (28) but, in contrast to (27), we define f as $f = f^* r_3^T r_3^*$. Then, Equation (33) becomes

$$\begin{aligned} \dot{\widetilde{v}}_Q &= -\frac{f^* r_3 r_3^T r_3^*}{m_Q} + ge_3 - \dot{v}_Q^* \\ &= \frac{f^*}{m_Q}\Pi_{r_3} r_3^* + ge_3 - \dot{v}_Q^* - \frac{f^*}{m_Q} r_3^* \end{aligned} \tag{35}$$

Adopting the time-scale separation approximation, we may analyse the translational and rotational systems in different time-scales. Thus, we may assume that we have the UAV oriented as desired, since the attitude loop converges much faster than the translational. This means that $r_3 = r_3^*$ and so $\Pi_{r_3} r_3^* = 0$. Under this assumption, the desired thrust vector input $f^* r_3^*$ can be written as

$$f^* r_3^* = m_Q(K_p \widetilde{x}_Q + K_v \widetilde{v}_Q + ge_3 - \dot{v}_Q^*) \tag{36}$$

And so, (35) becomes

$$\dot{\widetilde{v}}_Q = -K_p \widetilde{x}_Q - K_v \widetilde{v}_Q - \frac{f^*}{m_Q}\Pi_{r_3}\widetilde{r}_3 \tag{37}$$

where $\widetilde{r}_3 = (r_3 - r_3^*)$. The system controlled by (36) is, then

$$\begin{cases} \dot{\widetilde{x}}_Q = \widetilde{v}_Q & (38) \\ \dot{\widetilde{v}}_Q = -K_p \widetilde{x}_Q - K_v \widetilde{v}_Q + \widetilde{u} & (39) \end{cases}$$

where $\widetilde{u} = -\dfrac{f^*}{m_Q}\Pi_{r_3}\widetilde{r}_3$.

This system can be represented in the form of $\dot{X} = AX + B\widetilde{u}$, with $X = [\widetilde{x}^T \ \ \widetilde{v}^T]^T$ and $B = [0_{3\times 3} \ \ I_{3\times 3}]^T$. Matrix A is negative definite for any positive gains K_p and K_v, so the system is exponentially stable for $\widetilde{U} = 0$. To prove the stability of the system, we define the Lyapunov function $S = \frac{1}{2}X^T P X$, where $P \in \mathbb{R}^{6\times 6}$ is a positive definite symmetric matrix, which verifies Lyapunov equation $\frac{1}{2}(A^T P + PA) + Q = 0$. Q is also a positive definite symmetric matrix in $\mathbb{R}^{6\times 6}$.

We can bound the defined Lyapunov function by the following values

$$\frac{1}{2}\lambda_m(P)||X||^2 \leq S \leq \frac{1}{2}\lambda_M(P)||X||^2 \tag{40}$$

with $\lambda_m(P)$ and $\lambda_M(P)$ being, respectively, the minimum and maximum eigenvalues of the matrix P. The derivative of S is given by $\dot{S} = -X^T Q X + \widetilde{U}^T P X$. The Cauchy-Schwarz and triangular inequalities can be used to bound this expression

$$\begin{aligned} \dot{S} \leq -\lambda_m(Q)(||\widetilde{x}_Q||^2 + ||\widetilde{v}_Q||^2) \\ + \lambda_M(P)\frac{f^*}{m_Q}||\Pi_{r_3}\widetilde{r}_3||\ (||\widetilde{x}_Q|| + ||\widetilde{v}_Q||) \end{aligned} \tag{41}$$

For the attitude control, we use the following Lyapunov function

$$L = \frac{1}{2}\widetilde{r}_3^T\widetilde{r}_3 = \frac{1}{2}(r_3 - r_3^*)^T(r_3 - r_3^*) \tag{42}$$

with time derivative given by

$$\dot{L} = \widetilde{r}_3^T\dot{\widetilde{r}}_3 = (r_3 - r_3^*)^T(\dot{r}_3 - \dot{r}_3^*) \tag{43}$$

Since $r_3^* = \dfrac{f^* r_3^*}{||f^* r_3^*||} = \dfrac{F^*}{f^*}$, its derivative will be

$$\dot{r}_3^* = \Pi_{r_3^*}\frac{\dot{F}^*}{f^*} = \Pi_{r_3^*}\frac{m_Q(K_p\widetilde{v}_Q + K_v\dot{\widetilde{v}}_Q - \ddot{v}_Q^*)}{f^*} \tag{44}$$

Using (39), $\dot{r}_3^*$ finally becomes

$$\dot{r}_3^* = \frac{\Pi_{r_3^*} m_Q}{f^*}(b + K_v\widetilde{u} - \ddot{v}_Q^*) \tag{45}$$

with $b = -K_v K_p \widetilde{x}_Q + (K_p - K_v^2)\widetilde{v}_Q$. Replacing $\dot{r}_3$ and $\dot{r}_3^*$ in (43), we obtain

$$\dot{L} = -\widetilde{r}_3^T S(r_3)\left(R\Omega - S(r_3^*)\frac{m_Q}{f^*}b + K_v\widetilde{u} - D^2 v_Q^*\right) \tag{46}$$

Using the following control input

$$\Omega = -R^T\left(\frac{1}{\epsilon}S(r_3)\widetilde{r}_3 + \frac{m_Q}{f^*}S(r_3^*)\ddot{v}_Q^*\right) \tag{47}$$

where ϵ is the tuning gain used to enforce the time-scale separation, $\dot{L}$ becomes

$$\begin{aligned} \dot{L} = -\frac{1}{\epsilon}\widetilde{r}_3^T\Pi_{r_3}^2\widetilde{r}_3 + \widetilde{r}_3^T S(r_3)\Pi_{r_3}S(r_3^*)\frac{m_Q}{f^*}b \\ - K_v\widetilde{r}_3^T S(r_3)\Pi_{r_3}S(r_3^*)\Pi_{r_3}\widetilde{r}_3 \end{aligned} \tag{48}$$

Using the triangular and Cauchy-Schwarz inequalities, we can bound $\dot{L}$ by

$$\dot{L} \leq -\left(\frac{1}{\epsilon} + K_v\right) ||\Pi_{r_3}\widetilde{r}_3||^2 + ||\Pi_{r_3}\widetilde{r}_3|| \frac{m_Q}{f^*}(K_p K_v ||\widetilde{x}_Q|| + |K_p - K_v^2|\ ||\widetilde{v}_Q||) \quad (49)$$

To analyse the stability of the global system, we start by defining a global Lyapunov function $V = S + L$. To have a simpler formula for the derivative of V, we define the following positive coefficients, which are upper bounds to the coefficients of the terms of $\dot{S}$ and $\dot{L}$. We assume that f^* is positive and finite, which with further analysis can be guaranteed by imposing restriction on the initial conditions of the system.

$C_0 = \lambda_m(Q)$, $C_1 = \lambda_M(P)\frac{f_M^*}{m_Q}$, $C_2 = \frac{m_Q K_p K_v}{f_m^*}$ and $C_3 = \frac{m_Q |K_p - K_v^2|}{f_m^*}$.

f_M^* and f_m^* are, respectively, the maximum and minimum values of f^*. Considering $||Y|| = ||\Pi_{r_3}\widetilde{r}_3||$, we can bound $\dot{V} = \dot{S} + \dot{L}$ as $\dot{V} \leq -\chi^T \Sigma \chi$, with $\chi = [||\widetilde{x}_Q||\ \ ||\widetilde{v}_Q||\ \ ||Y||]^T$ and

$$\Sigma = \begin{bmatrix} C_0 & 0 & -\frac{C_1 + C_2}{2} \\ 0 & C_0 & -\frac{C_1 + C_3}{2} \\ -\frac{C_1 + C_2}{2} & -\frac{C_1 + C_3}{2} & \frac{1}{\epsilon} + K_v \end{bmatrix}$$

It follows that, if Σ is positive definite, then the error system has an exponentially stable equilibrium point at the origin. One way to show that Σ is positive definite is by using Schur's complement condition for positive definiteness [4]. From there, we obtain the following upper bound on ϵ

$$\epsilon < \frac{4C_0}{(C_1 + C_2)^2 + (C_1 + C_3)^2 - 4C_0 K_v} \quad (50)$$

4. Load Position Control

The same approach used on Section 3 can be adopted to the system consisting of a quadrotor with an attached load. We start with the design of a Nonlinear Backstepping Controller, and afterwards a Hierarchical Controller is derived.

4.1. Nonlinear Backstepping Controller

As it was seen on Section 2.2, the dynamics equations for the system quadrotor-load can be split in three parts. Due to the particular form of the equations, it is possible to actuate on each one of these groups independently, by working at different time-scales for each subsystem.

The last group is used to give the desired attitude to the quadrotor, i.e. the desired vector Re_3. This can be achieved by actuating on the angular velocity Ω. With the quadrotor oriented as desired, i.e. neglecting the fast attitude dynamics, it is possible to use the component of $F = fr_3^*$ which is orthogonal to the vector q, in order to obtain a desired position of the load in relation to the quadrotor. In other words, this component of F may be used to control vector q. Finally, with $r_3 = Re_3$ and q in place, i.e. assuming that the attitude and cable dynamics are much faster than the load position dynamics, the component of F in the direction of q is used to control the position of the load.

We start with load position control, and use the following control input, in the direction of q

$$F_1 = -q(m_Q l \omega^T \omega + \alpha(m_Q + m_L)) \quad (51)$$

With F in this form, v_L is controlled by actuating on q. Since it is not possible to actuate directly in this vector, a desired q^* must be found. Assuming for now that $q = q^*$ and $r_3 = r_3^*$, if we choose $\alpha q^* = u - ge_3$, this subsystem is transformed into

$$\begin{cases} \dot{x}_L = v_L & (52) \\ \dot{v}_L = u & (53) \end{cases}$$

which is a double integrator system. In order to be able to follow trajectories, we may use the following u

$$u = -K_p \widetilde{x}_L - K_v \dot{\widetilde{x}}_L + D^2 x_L^* \quad (54)$$

where $\widetilde{x}_L = (x_L - x_L^*)$ and x_L^* is the desired load position. Expressions for q^* and for α are found solving $\alpha q^* = u - ge_3$. We obtain

$$q^* = -\frac{(u - ge_3)}{||u - ge_3||} \quad (55)$$

$$\alpha = -||u - ge_3|| \quad (56)$$

The negative solution for q^* is chosen because we want this vector to point downwards, i.e. have a positive third component, when $u = 0$.

The next control objective is to drive q to q^*, i.e. to control the relative position of the load. Recalling (7) and (16), it becomes clear that only the component of F orthogonal to q, denoted here by F_2, has an effect on the dynamics of q.

Lyapunov stability theory shows that the following control laws stabilize this part of the system

$$\omega^* = K_q S(q) q^* + S(q^*)\dot{q}^* \quad (57)$$

$$F_2 = -m_Q l S(q)^2 (q^* + S(\dot{q})(\omega - \omega^*) - S(q)\dot{\omega}^* + K_\omega S(q)(\omega - \omega^*)) \quad (58)$$

where K_q and K_ω are positive gains and $\dot{\omega}*$ is given by

$$\dot{\omega}^* = K_q(S(\dot{q})q^* + S(q)\dot{q}^*) + S(q^*)D^2 q^* \quad (59)$$

Meaning that expressions for the first and second derivatives of q^* have to be found. Given that q^* is a unit vector

$$\dot{q}^* = \Pi_{q^*} \frac{\dot{U}}{||U||} \tag{60}$$

$$D^2 q^* = -(2\dot{q}^* {\dot{q}^*}^T + q^* {\dot{q}^*}^T) \frac{\dot{U}}{||U||} + \Pi_{q^*} \frac{D^2 U}{||U||} \tag{61}$$

$\dot{U}$ and D^2U depend on $\dot{v_L}$ and $D^2 v_L$, while $\dot{v_L}$ and $D^2 v_L$ depend on the thrust force f, with components F_1 along q and F_2 orthogonal to q. Substituting these derivatives in (58) shows that F_2 depends on itself and we are in the presence of an algebraic loop. To avoid the algebraic loop, we assume that r_3 can be approximated by r_3^* , which means that $\dot{v}_L = \alpha q + g e_3$ and its derivative is $D^2 v_L = \dot{\alpha} q + \alpha \dot{q}$, with $\dot{\alpha} = \frac{\partial}{\partial t}(-||u - g e_3||) = -(u - g e_3)^T \dot{u}$.

The attitude control of the quadrotor is done by actuating in Ω. This control input has the same structure as the one designed in Section 3.1, given by Equation 30. The difference from the previous controller is the value of r_3^*. Here, it is given by

$$r_3^* = \frac{F}{f} \tag{62}$$

Its derivative is

$$\dot{r_3^*} = \Pi_{r_3^*} \frac{\dot{F}}{f} = \Pi_{r_3^*} \frac{\dot{F_1} + \dot{F_2}}{f} \tag{63}$$

The derivative of F_1 is

$$\dot{F_1} = -S(\omega) F_1 - q(2 m_Q l \omega^T \dot{\omega} + \dot{\alpha}(m_Q + m_L)) \tag{64}$$

And the derivative of F_2 is

$$\begin{aligned} \dot{F_2} = \quad & 2 m_Q l S(q) \omega q^T (q^* + S(\dot{q})(\omega - \omega^*)) \\ & - m_Q l S(q)^2 (\dot{q}^* + (S(D^2 q) + K_\omega S(\dot{q}))(\omega - \omega^*)) \\ & - m_Q l S(q)^2 ((S(\dot{q}) + K_\omega S(q))(\dot{\omega} - \dot{\omega^*}) \\ & - S(\dot{q}) \dot{\omega^*} - S(q) D^2 \omega^*)) \end{aligned} \tag{65}$$

4.2. Hierarchical Nonlinear Controller

In this section, a hierarchical nonlinear controller is designed, based on the time-scale separation principle. It will be shown that with this controller, we can stabilize an adequately defined error system for the suspended load control problem. Although it will not be quantified how high the inner loop gains need to be with respect to the outer loop gains.

We start with the stabilization of the translational equations. Using the time-scale separation principle, the control input can be designed assuming $r_3 = r_3^*$, so

$$F_1 = f r_3^* = -q(m_Q l \omega^T \omega + \alpha(m_Q + m_L)) \tag{66}$$

So the dynamics of v_L becomes

$$\dot{v}_L = \alpha q + g e_3 + u_1 \tag{67}$$

With $u_1 = -\frac{1}{m_Q + m_L} q^T f (r_3 - r_3^*) q$.

Defining $\dot{\widetilde{v}}_L = \dot{v}_L - \dot{v}_L^*$, the equation can be transformed into

$$\dot{\widetilde{v}}_L = \alpha q^* + g e_3 - \dot{v}_L^* + \widetilde{u} \tag{68}$$

With $\widetilde{u} = u_1 + \alpha(q - q^*)$.

Using the following control law

$$\alpha q^* = -K_p \widetilde{x}_L - K_v \widetilde{v}_L - g e_3 + \dot{v}_L^* \tag{69}$$

the system becomes

$$\begin{cases} \dot{\widetilde{x}}_L = \widetilde{v}_L & (70) \\ \dot{\widetilde{v}}_L = -K_p \widetilde{x}_L - K_v \widetilde{v}_L + \widetilde{u} & (71) \end{cases}$$

which is a stable system for $K_p, K_v > 0$ and $\widetilde{u} = 0$.

Since q^* is an unit vector, we take the following conclusions from Equation (69)

$$q^* = \frac{-(-K_p \widetilde{x}_L - K_v \widetilde{v}_L - g e_3 + \dot{v}_L^*)}{||-K_p \widetilde{x}_L - K_v \widetilde{v}_L - g e_3 + \dot{v}_L^*||} \tag{72}$$

$$\alpha = -||-K_p \widetilde{x}_L - K_v \widetilde{v}_L - g e_3 + \dot{v}_L^*|| \tag{73}$$

We tackle now the problem of controlling the position of the load in relation to the quadrotor. In other words, we design a control law to drive q to q^*. Introducing $\epsilon_1 \in [0, 1]$ to formalize time-scale separation and using the control input

$$\omega^* = -\frac{1}{\epsilon_1} S(q) \widetilde{q} = \frac{1}{\epsilon_1} S(q) q^* \tag{74}$$

The equation of dynamics of q becomes

$$\epsilon_1 \dot{q} = -S(q)^2 q^* - \epsilon_1 S(q) \widetilde{\omega} \tag{75}$$

Defining the Lyapunov Function

$$V_1 = \frac{1}{2}(q - q^*)^T (q - q^*) \tag{76}$$

Its derivative is given by

$$\dot{V_1} = -\frac{1}{\epsilon_1} {q^*}^T S(q)^T S(q) q^* + {q^*}^T S(q) \widetilde{\omega} \tag{77}$$

where $\dot{q}^*$ was assumed to be null, due to the separation principle. It is assumed that the response of the inertial translation loop is much slower than this one, so the desired q position is approximately constant.

To guarantee the stability of the global systems, we define the following Lyapunov equation

$$V_2 = V_1 + \frac{1}{2} \widetilde{\omega}^T S(q)^T S(q) \widetilde{\omega} \tag{78}$$

with derivative given by

$$\begin{aligned} \dot{V_2} = & -\frac{1}{\epsilon_1} {q^*}^T S(q)^T S(q) q^* + \widetilde{\omega}^T S(q)^T \\ & \left(q^* + S(\dot{q}) \widetilde{\omega} - S(q) \dot{\omega}^* - \frac{f r_3^*}{m_Q l} \right) \end{aligned} \tag{79}$$

Using the following control law

$$F_2 = f r_3^* = -m_Q l S(q)^2 \left(q^* + S(\dot{q})\widetilde{\omega} - S(q)\dot{\omega}^* + \frac{K_\omega}{\epsilon_1} S(q)\widetilde{\omega} \right) \quad (80)$$

with $\dot{\omega}^* = \frac{1}{\epsilon_1} S(\dot{q}) q^*$, $\dot{V}_2$ becomes

$$\dot{V}_2 = -\frac{1}{\epsilon_1} {q^*}^T S(q)^T S(q) q^* - K_\omega \widetilde{\omega}^T S(q)^T S(q) \widetilde{\omega} \quad (81)$$

From this expression we see that $\dot{V}_2 < 0$ for any positive ϵ_1 and K_ω, so we have stability for the given control law.

For the quadrotor attitude control, we will actuate on Ω to take vector r_3 to the desired position.

The Lyapunov function to be used is

$$L = \frac{1}{2} \widetilde{r}_3^T \widetilde{r}_3 \quad (82)$$

Its derivative is given by

$$\dot{L} = \widetilde{r}_3^T \dot{\widetilde{r}}_3 = (r_3 - r_3^*)^T (\dot{r}_3 - \dot{r}_3^*) \quad (83)$$

where $\dot{r}_3^*$ is assumed to be null due to the separation principle. This control loop is assumed to be much faster than the ones discussed previously, so the desired attitude of the quadrotor is assumed to be constant inside this loop. So $\dot{L}$ becomes

$$\dot{L} = (r_3 - r_3^*)^T (-S(r_3) R \Omega) = {r_3^*}^T S(r_3) R \Omega \quad (84)$$

The control input is, then

$$\Omega = \frac{1}{\epsilon_2} R^T S(r_3) r_3^* \quad (85)$$

that transforms $\dot{L}$ into

$$\dot{L} = -\frac{1}{\epsilon_2} {r_3^*}^T S(r_3)^T S(r_3) r_3^* \quad (86)$$

The stability is achieved for any $\epsilon_2 > 0$.

Given that each of the decoupled subsystems is exponentially stable, it can be shown that for sufficiently small ϵ_1 and ϵ_2, the overall system is exponentially stable, resorting to arguments from singular perturbation theory [5].

5. Simulation Results

In this section, the simulation results, obtained with the load position controller designed using the backstepping technique, are shown and discussed.

A saturation function for the error was used in order to avoid high control inputs. The gains used for the simulations are the same as the ones used in the experimental part, discussed further ahead. The values used for the quadrotor position control are $K_p = 8$, $K_v = 4$ and $K_\Omega = 7$. For the load position controller, they are $K_p = 16$, $K_v = 2.5$, $K_q = 9$, $K_\omega = 1.5$ and $K_{r_3} = 7$.

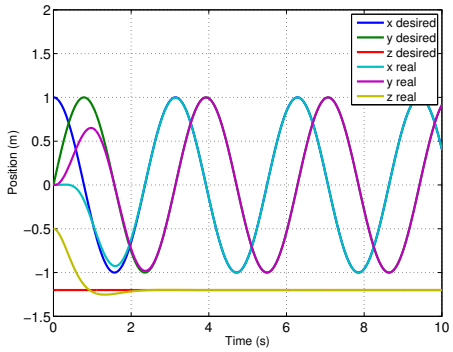

Figure 2: Quadrotor circular trajectory response.

For the circular trajectory simulation, the path has a radius of 1 meter, and the desired speed is equal to 2 m/s. The UAV start in $x_Q(0) = [0 \;\; 0 \;\; -0.5]^T$. The results for the quadrotor alone are shown in Figure 2.

The step response of the quadrotor with a load attached is shown in Figure 3.

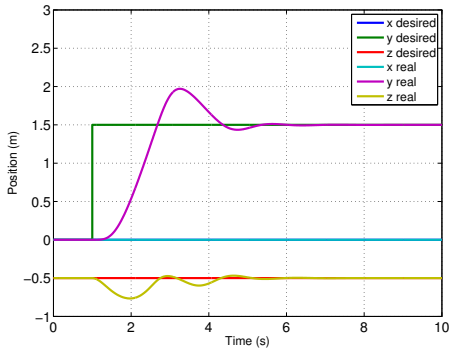

Figure 3: Load position controller step response.

The step occurs after one second of simulation and, 5 seconds later, the quadrotor is steady on the desired position. It has an overshoot of almost 33%, and, right after the step, the UAV rises almost 30 cm. This happens to keep the vector q pointing downwards. A different choice of gains would make the rising height smaller.

The circular trajectory tracking results are shown in Figure 4.

6. Experimental Results

In this section, the experimental results obtained are presented. The controllers used were the Backstepping Nonlinear Controllers and the videos of the trials illustrated in this section are available at [1].

The tests were made in the Sensor-based Cooperative Robotics (SCORE) Laboratory from the University of Macau, in Macau, China. This laboratory is equipped with a Vicon Bonita Motion Capture System which, through the use of 12 cameras, is able to accurately measure the position and orientation of an object that contains spherical reflectors. Given the

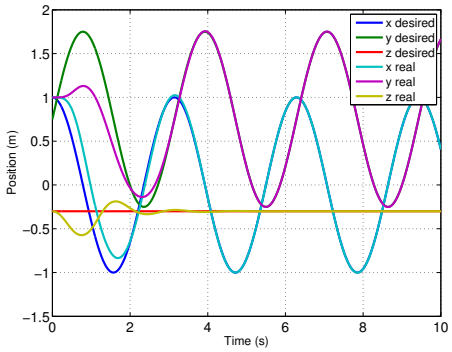

Figure 4: Load position controller, circular trajectory tracking response.

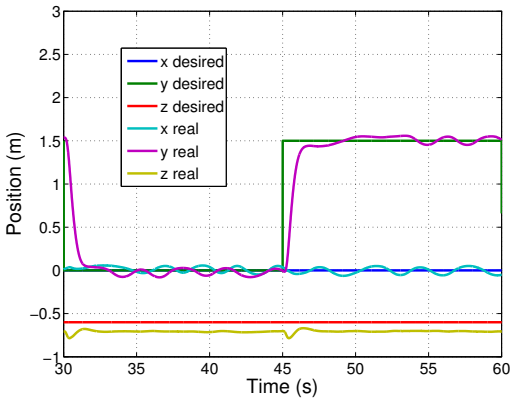

Figure 5: Experimental results obtained for the quadrotor position control, in response to setpoints.

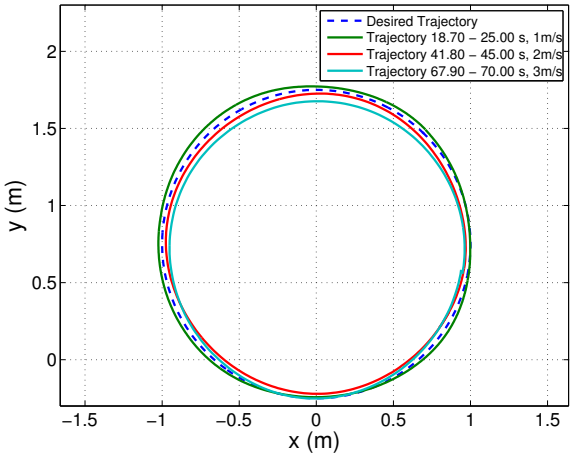

Figure 6: Top view of the trajectory, for different speeds.

sub-millimetre and sub-degree accuracy of the position and attitude measurements, simple first-order backward difference approximations can be used to obtain linear and angular velocity estimates with low levels of noise. The reflectors used for the capture system were strategically positioned, both in the quadrotor and in the load. Data was collected and sent to the controller at a rate of 100Hz. The UAV model used was a Blade 200 QX, which weights approximately 210g, including the battery. The total load weight was 60g, and the cable, made of carbon fiber tubes, had a length of 33cm. The flight control system was running off-board. A desktop computer running Matlab and Simulink was receiving data from Vicon and processing the control algorithm in real-time. It also converted the outputs of the controller, in S.I. units, to values of voltage to be sent to the quadrotor. These values were sent using an XBee wireless link, at a rate of 50 Hz.

We start with the tests done for the quadrotor position control, without any load attached, using the Backstepping Nonlinear Controller.

The results obtained are shown in Figure 5. The response shows a settling time of approximately 2 seconds for a step amplitude of 1.5m. When the UAV reaches the destination, it oscillates in a range of approximately 10cm. There is a static error in the z direction, constant along the whole test. It is very likely that this happened because the mass of the quadrotor used in the controller is different from the real one. This could be solved by using an integrator in this direction.

To test the trajectory tracking performance of the controller, a circular course was used. The test started with a low linear velocity of 1m/s and, after a while, it increased suddenly to higher value - 2 m/s, 2.5 m/s and finally 3 m/s. After that the speed decreased slowly until the UAV stopped. The top view trajectories for different speeds are shown in Figure 6. Position error can be seen in Figure 7.

A static error in the z direction of approximately 10 cm is present once again, what suggests, one more time, that the mass used in the controller was different from the real one. The norm of the position error was generally below 20 cm. This decreases to 10 cm if we disregard the static error in the z direction. As the desired linear speed increases, the UAV trajectory tends to do a turn with lower radius, what happens because the quadrotor does not have enough thrust to compensate the higher acceleration. As expected, the position error also becomes higher.

For the load position control, the same tests used for the quadrotor alone are repeated. However, for the setpoint analysis, we do tests using the quadrotor position controller and using the load position controller. The results are compared afterwards. For the trajectory tracking analysis, just the load position controller is used. Different values of speed are tested.

To be able to compare the performances of the quadrotor and load controllers, we can check the plots shown in Figures 8 and 9, where we can see, respectively, the components of the error and the components of vector q. The x component of q is not represented.

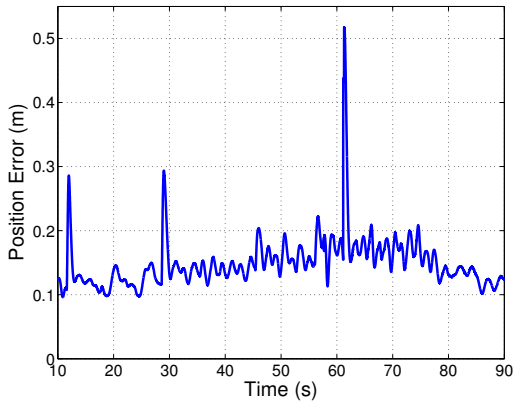

Figure 7: Magnitude of the error for the quadrotor following a circular trajectory.

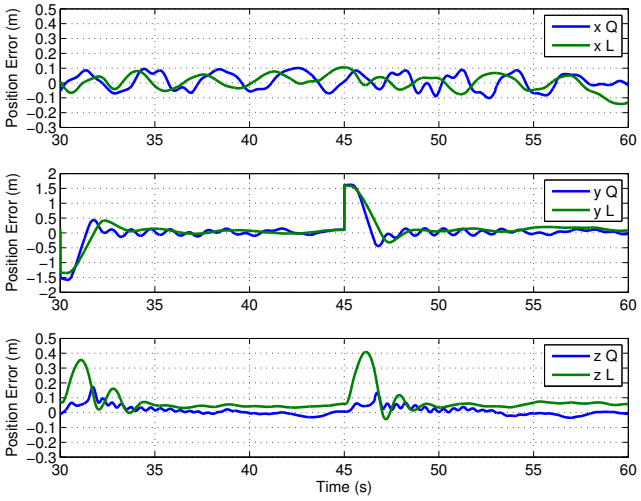

Figure 8: Comparison of the error for the different components.

The settling time is lower for the load position controller, as it takes less time to damp the sinusoid oscillations. When the UAV reaches its destination, the load keeps swinging. With the quadrotor controller, it oscillates in a range of approximately 20 cm, while with the load controller this range is of approximately 15 cm. The oscillation frequency is much higher and the rate of decay much smaller, with quadrotor position controller. The norm of the position error is similar in both situations, but oscillates with a lower frequency for the load position control.

Analysing the comparison of each component of the error we see that the major differences are in the y and z components. x component was supposed to be null during the tests, and so what we observe in the plot is mostly the effect of external disturbances.

We observe lower frequency oscillation in y and z components for the load controller. We also observe that the z position error is much higher with load controller, right after the step input. In fact, with this

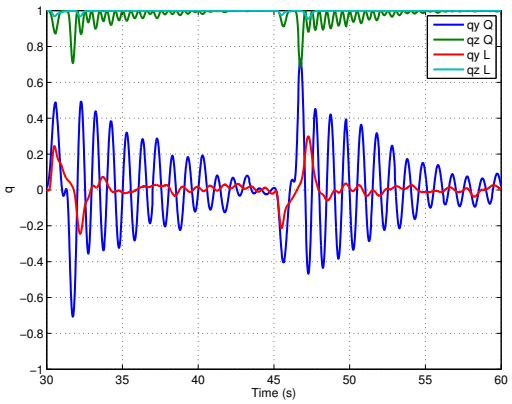

Figure 9: Comparison of the vector q components.

controller, the UAV increased its height while moving the load from one point to another.

While using the load position controller, the UAV rises when moving from one point to another. This is done to avoid high swings in the load, and to keep vector q pointing downwards. This can be confirmed by Figure 9, where we see that vector q barely changes comparing to the case where quadrotor controller is used. If we compute the root mean square (RMS) error of vector q in relation to the vertical position we obtain lower results when using the load position controller - the RMS using quadrotor position controller is 0.2116 and 0.0497 for y and z directions, respectively, while for the load position control we have 0.0618 in y and 0.0067 in z.

For the circular trajectory the tests started with a linear speed of 0.5 m/s, and increased in steps of 0.5 m/s until it reached 2 m/s. Trajectories for different speeds are shown in Figure 10, and position errors and desired velocity are shown of Figure 11.

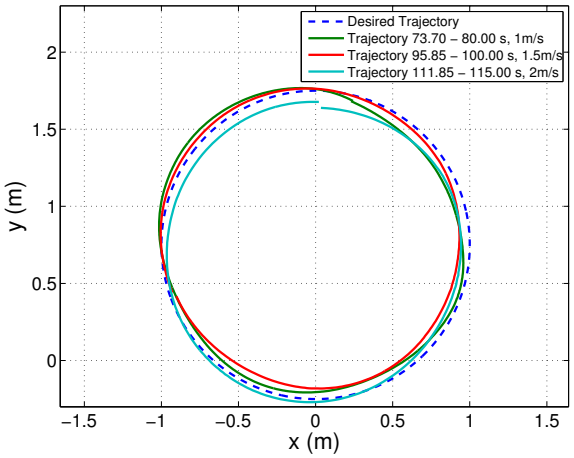

Figure 10: Top view of the trajectory, for different speeds.

We see that the norm of the position error stayed mostly below the 20 cm mark, with peaks happening

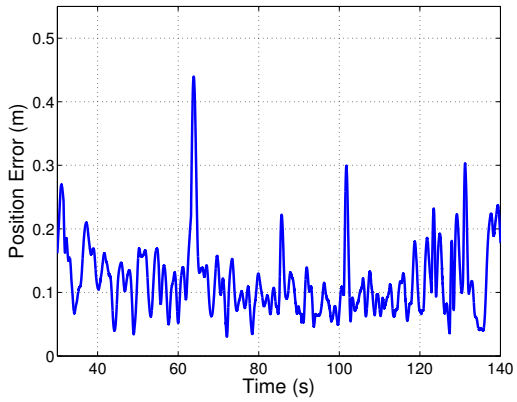

Figure 11: Magnitude of the error using load position controller, following a circular trajectory.

when the step occurred. The position error did not change significantly with the increase of desired velocity. Maybe these changes would be noted for higher speeds.

7. Final Remarks

The structure of the equations of motion for the multibody system was crucial in the design of the controllers for this system. It was possible to split these equations in three different groups, and actuate in each one of them independently. The component of thrust perpendicular to the cable was used to control the position of the load in relation to the quadrotor, while the component in the direction of the cable was used to control the position of the load in an inertial reference frame.

The controllers performances were tested both in simulations and in real experiments. Load transportation using the quadrotor position controller, and considering the load as a disturbance, was compared with the use of the controller which takes into account the dynamics of the load. This last one showed less swing of the cable, mainly in terms of oscillation frequency and settling time.

7.1. Future Work

The results obtained with this research are just a base for future developments. Some topics that could give continuation to this work are (a) Experimentally test the Hierarchical controllers developed. (b) Generalize the dynamic models derived, to be able to be applied to different scenarios. This includes considering the load as a rigid body, that the connecting cable can bend or that the cable is not connected directly to the centers of gravity of the bodies. (c) Consider the problem of having one load being transported by a group of cooperating UAVs, and generalize the controllers designed here for that case. (d) Combine the developed controller with adaptive control techniques, in order to reject external disturbances such as the presence of wind or model mismatches such as imperfect knowledge of the load mass.

References

[1] Load transportation using rotary-wing uavs - experimental trials. `http://web.tecnico.ulisboa.pt/rafael.j.f.santos/msc_thesis_videos.php`. Accessed: 2015-11-04.

[2] M. Bernard and K. Kondak. Generic slung load transportation system using small size helicopters. In *Robotics and Automation, 2009. ICRA'09. IEEE International Conference on*, pages 3258–3264. IEEE, 2009.

[3] S. Bertrand, N. Guénard, T. Hamel, H. Piet-Lahanier, and L. Eck. A hierarchical controller for miniature vtol uavs: design and stability analysis using singular perturbation theory. *Control Engineering Practice*, 19(10):1099–1108, 2011.

[4] R. W. Cottle. Manifestations of the schur complement. *Linear Algebra and its Applications*, 8(3):189–211, 1974.

[5] H. K. Khalil. *Nonlinear Systems*. Prentice Hall, 3^{rd} edition edition, 2000. ISBN:0-13-122740-8.

[6] T. Lee, M. Leoky, and N. H. McClamroch. Geometric tracking control of a quadrotor uav on se (3). In *Decision and Control (CDC), 2010 49th IEEE Conference on*, pages 5420–5425. IEEE, 2010.

[7] J. Li and Y. Li. Dynamic analysis and pid control for a quadrotor. In *Mechatronics and Automation (ICMA), 2011 International Conference on*, pages 573–578. IEEE, 2011.

[8] Q. Lindsey, D. Mellinger, and V. Kumar. Construction with quadrotor teams. *Autonomous Robots*, 33(3):323–336, 2012.

[9] D. Mellinger, M. Shomin, N. Michael, and V. Kumar. Cooperative grasping and transport using multiple quadrotors. In *Distributed autonomous robotic systems*, pages 545–558. Springer, 2013.

[10] I. Palunko, P. Cruz, and R. Fierro. Agile load transportation: Safe and efficient load manipulation with aerial robots. *Robotics & Automation Magazine, IEEE*, 19(3):69–79, 2012.

[11] I. Palunko, R. Fierro, and P. Cruz. Trajectory generation for swing-free maneuvers of a quadrotor with suspended payload: A dynamic programming approach. In *Robotics and Automation (ICRA), 2012 IEEE International Conference on*, pages 2691–2697. IEEE, 2012.

[12] K. Sreenath, T. Lee, and V. Kumar. Geometric control and differential flatness of a quadrotor uav with a cable-suspended load. In *Decision and Control (CDC), 2013 IEEE 52nd Annual Conference on*, pages 2269–2274. IEEE, 2013.